JOURNAL OF MATERIALS SCIENCE 22 (1987) 3611–3614

Structural properties of non-stoichiometric zinc oxide films

M. J. BRETT
Department of Electrical Engineering, The University of Alberta, Edmonton, Alberta T6G 2G7, Canada

R. R. PARSONS
Department of Physics, The University of British Columbia, Vancouver V6T 1W5, Canada

We report a study of the crystal structure and microstructure of sputtered non-stoichiometric ZnO_x thin films for which $0.7 < x < 1$. A substrate r.f. discharge was used to control film stoichiometry during deposition. All films had a columnar microstructure, and the film surface progressed from rough to smooth with increased oxidation. X-ray diffraction analysis detected no presence of crystalline zinc in any film. The crystallite size, strain and orientation of ZnO, detected in all films, was dependent on film composition and substrate r.f. discharge power. A model of film structure incorporating the competing effects of ion bombardment (causing amorphization) and increased oxygen content (creating improved crystallinity and orientation) is used to explain the observed variation of ZnO_x crystal structure.

1. Introduction

ZnO is a large-bandgap semiconductor that exhibits a high conductivity if doped by oxygen deficiency, is transparent, and has a large electromechanical coupling coefficient. These properties have led to applications of thin films of ZnO as transparent conductors [1], transparent window insulation [2], gas sensors [3], and as the piezoelectric film in surface acoustic wave devices [4]. To optimize ZnO films for these applications, control of composition, transparency, conductivity and crystal structure is essential.

In earlier work [5] we have reported in detail the electrical and optical properties of sputter-deposited ZnO_x films as a function of composition for $0.7 < x < 1$. Films produced at composition $ZnO_{0.95}$ were excellent transparent conductors of resistivity $1.9 \times 10^{-3}\,\Omega\,cm$. In this paper we report the crystalline and microstructural properties of ZnO_x as determined by X-ray diffraction and scanning electron microscopy (SEM). These structural properties are correlated with film composition and deposition process variables.

2. Experimental procedure

ZnO thin films of nominal thickness $0.8\,\mu m$ were deposited on uncooled Corning 7059 glass substrates using a high-rate, modified d.c. planar magnetron technique described in detail previously [2]. In this technique a zinc target was reactively sputtered in a 1 Pa $Ar–O_2$ discharge with the O_2 partial pressure maintained at 0.05 Pa to keep the target surface free of oxide. Sputtered metal atoms were oxidized at the substrate with control of film stoichiometry achieved by an applied r.f. discharge at the substrate. Rutherford backscattering analysis of film stoichiometry showed that the effect of the r.f. discharge was to increase the O/Zn composition ratio [6]. Enhanced film oxidation resulted from increased r.f. discharge power, through the mechanisms of preferential resputtering and evaporation of zinc and by activation and ion plating of oxygen species. The power of the r.f. discharge was monitored by the d.c. self-bias voltage that occurred at the substrate. A set of films of stoichiometries $ZnO_{0.76}$ to ZnO was produced by sequentially increasing the power of the substrate r.f. discharge. Power densities at the substrate ranged from 0 to $30\,mW\,cm^{-2}$. At zero applied r.f. power, the substrate floated to a self-bias of -6 V, due to the characteristics of the d.c. magnetron discharge.

ZnO_x films deposited by this technique receive low-energy (less than 140 eV) positive ion bombardment due to the substrate r.f. discharge and have a composition dependent on the power of the discharge. It was expected that both film composition and the energy of ion bombardment would play a role in determining the ZnO_x crystal structure. In an attempt to separate and identify the effects of bombardment-induced structural changes from those of composition-related structural changes, two further experiments were performed.

First, a set of stoichiometric films (composition ZnO) was produced by sputtering in pure oxygen. These films were also exposed to sequentially increasing power levels of the substrate r.f. discharge. Thus, these films experienced ion bombardment but no stoichiometry change.

In the second experiment, a set of films was deposited at varied O_2 partial pressure levels in the sputter chamber, but without a substrate discharge, yielding ZnO_x films of varied composition that had no exposure to ion bombardment.

0022–2461/87 $03.00 + .12

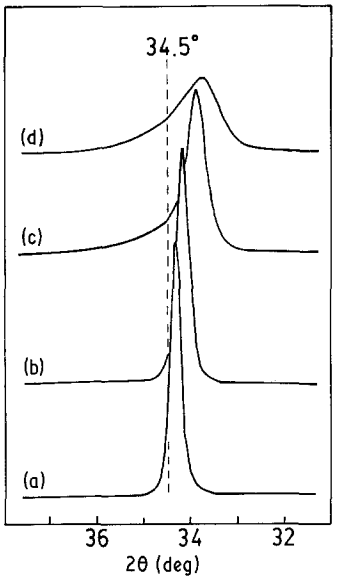

Figure 1 X-ray diffraction intensities of stoichiometric ZnO films, as a function of diffraction angle 2θ and substrate bias voltage during deposition. (a) ZnO-A, −6 V; (b) ZnO-B, −100 V; (c) ZnO-C, −150 V; (d) ZnO-D, −200 V.

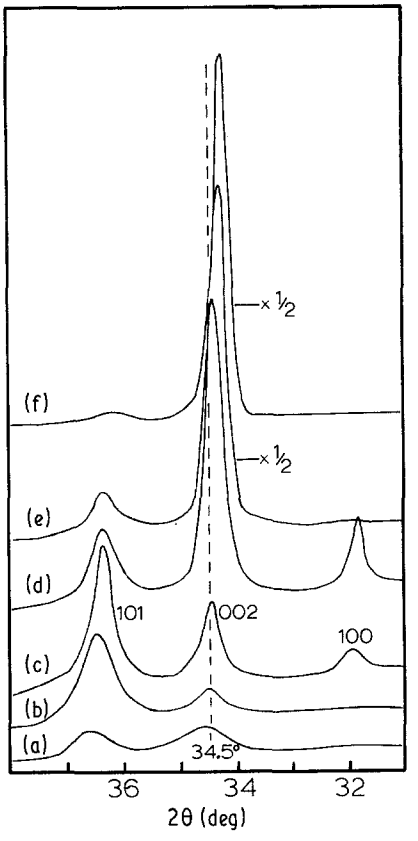

Figure 2 X-ray diffraction intensities of ZnO_x films deposited at various values of oxygen flow rate $f(O_2)$: (a) 1.0, (b) 1.4, (c) 1.8, (d) 2.2, (e) 2.6, (f) 3.0 s.c.c.m. ($cm^3\ min^{-1}$ at standard temperature and pressure).

3. Results

3.1. Effects of ion bombardment on film structure

Fig. 1 shows the X-ray diffraction spectra, using 0.154 nm Cu$K\alpha$ radiation, of the set of stoichiometric ZnO films produced with a substrate r.f. discharge. Only the 0 0 2 peak of the hexagonal wurtzite crystal structure is observed, indicating a strong orientation of the crystal c-axis perpendicular to the substrate. Film ZnO-A has lattice strain of 0.4%, calculated using the shift of the 0 0 2 peak to 34.30° from its unstrained value of 34.47°. Such strain and a preferred basal orientation are typically observed in sputtered ZnO coatings [7, 8].

The energy and flux of positive ion bombardment increase as the substrate bias becomes more negative. We have calculated that at a bias of −100 V, an ion bombardment flux of 3×10^{14} ions $cm^{-2}\,sec^{-1}$ occurs at ion energies distributed between 0 and 100 eV [6]. In comparison, the deposition rate of ZnO is 2×10^{15} atoms $cm^{-2}\,sec^{-1}$. From Fig. 1 it is observed that the primary effect of increased ion bombardment is a degradation of the crystallinity of the ZnO films. Lattice strain increases such that the position for the 0 0 2 peak in film ZnO-D is 33.78°, and significant broadening of the peak occurs. Similar effects of low-energy bombardment-induced amorphization have been observed in sputtered silver films [9] and silicon films [10].

3.2. Effects of composition on film structure

Fig. 2 shows X-ray diffraction spectra of ZnO_x films deposited without substrate bias but at increasing values of oxygen flow rate $f(O_2)$ to the deposition chamber. Rutherford backscattering analysis of the composition of these films was not performed. However, from the results of analysis on other films and extensive experience with ZnO film deposition, we estimate the compositions to vary from about $ZnO_{0.5}$ to $ZnO_{0.9}$ as $f(O_2)$ is increased. The hexagonal wurtzite diffraction peaks of ZnO are labelled in Fig. 2. Films deposited at low $f(O_2)$ display broad diffraction peaks of low intensities, indicative of a microcrystalline or near-amorphous material. No diffraction peaks of metallic zinc were identified, presumably due to the large disorder in the films. A similar lack of metal diffraction peaks was observed by Affinito *et al.* [11] for sputtered films of composition $AlN_{0.4}$ to AlN.

The primary effects of a change in composition from oxygen-deficient material towards stoichiometric ZnO are a domination of the 0 0 2 peak (indicating preferred basal orientation) and an increase in lattice strain. As expected, the film produced with a composition nearest to stoichiometric ZnO at $f(O_2) = 3.0$ has, qualitatively, the same structural characteristics as Film ZnO-A in Fig. 1.

3.3. Structure of bias-sputtered ZnO_x films

In Fig. 3 the diffraction spectra of bias-sputtered ZnO_x are given. Corresponding composition, grain-size and thickness data are given in Table I. The grain size was estimated from the broadening of the 0 0 2 peak using the Scherrer relation [12]. Some of the diffraction data may be explained using the results of Figs 1 and 2. Film ZnO-1 was deposited under the same conditions as the film at $f(O_2) = 2.2\ cm^3\ min^{-1}$ in Fig. 2, and has a similar diffraction spectrum. Film ZnO-6, with composition ZnO and bias voltage −140 V, should be and is similar to Film ZnO-D of Fig. 1; it is stoichiometric with associated lattice strain, but has suffered

TABLE I Properties of sputtered ZnO_x films

Film	Substrate bias (V)	Thickness (μm)	Composition O/Zn	Grain size (nm)
ZnO-1	−6	0.90 ± 0.03	0.76 ± 0.04	36 ± 15%
ZnO-2	−40	0.90	0.78	23
ZnO-3	−65	0.84	0.83	42
ZnO-4	−90	0.70	0.95	44
ZnO-5	−115	0.65	0.99	43
ZnO-6	−140	0.61	1.00	39

amorphization due to ion bombardment. We explain the progression of diffraction spectra for Films ZnO-4 to ZnO-6 as increased amorphization due to the increased energy and flux of ion bombardment.

Using our model of bombardment and composition effects on structure, we did not expect ion bombardment at the substrate bias voltages of −40 and −65 V to seriously degrade the crystallinity of Films ZnO-2 and ZnO-3. Instead, our model predicts that the composition change of $ZnO_{0.76}$ to $ZnO_{0.83}$ will create an improvement in crystallinity. Clearly the data do not agree with these predictions and at present we are unable to explain this progression of structure. It is

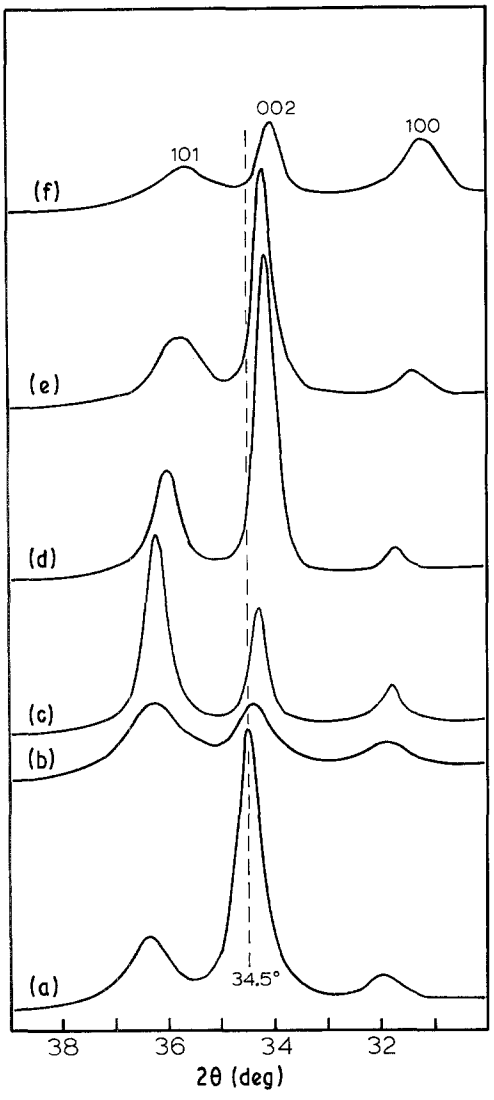

Figure 3 X-ray diffraction intensities of ZnO_x films deposited at various substrate bias voltages: (a) ZnO-1, −6 V; (b) ZnO-2, −40 V; (c) ZnO-3, −65 V; (d) ZnO-4, −90 V; (e) ZnO-5, −115 V; (f) ZnO-6, −140 V.

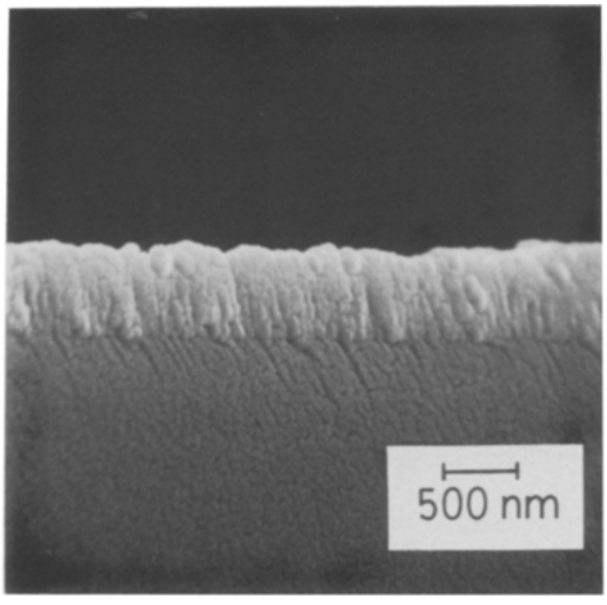

Figure 4 SEM photograph of a cleaved cross-section of Film ZnO-1 on a glass substrate. The fine structure visible on the glass is due to a thin overcoating of gold.

emphasized that the variation of diffraction spectra with bias is repeatable; nearly identical spectra were obtained from two other sets of ZnO_x films.

Similar anomalous transitions in structure have been observed by Hebard and Nakahara [13] in sputter-deposited $In–In_2O_3$ composites. As a function of increasing oxide component they observed a structural transition through an amorphous phase. Our data of Fig. 2 for increasing oxide component of ZnO_x do not show such a transition; however, the bias-sputtered ZnO_x data of Fig. 3 show a near-amorphous phase for Film ZnO-2. We hope that further study will provide an understanding of these data.

3.4. Structure investigation by SEM

Figs 4 and 5 show cross-sectional SEM photographs of Films ZnO-1 and ZnO-4 on glass substrates. A

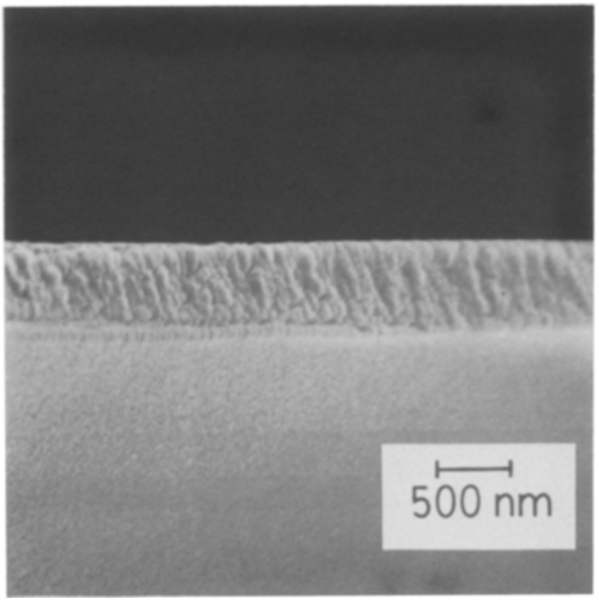

Figure 5 SEM photograph of a cleaved cross-section of Film ZnO-4 on a glass substrate.

columnar microstructure is evident in both films; however, Film ZnO-4 has a much smoother surface topography. This result is in agreement with observations by other workers that an increase in the oxide component of metal–metal oxide composites leads to a smoothing of the film surface [14]. Furthermore, ion bombardment of the growing film is known to sputter the film itself and redistribute film atoms [15], thus performing a smoothing process.

4. Conclusions

We have studied the microstructure and crystal structure of bias-sputtered ZnO_x films, where $0.7 < x < 1$. A columnar microstructure is observed in all films, and the film surface progresses from rough to smooth as the oxygen content is increased. The crystal structures of the ZnO_x films showed no presence of crystalline zinc, and most films had a preferred basal orientation of ZnO. A model of film structure incorporating the competing effects of ion bombardment (creating amorphization) and increased film oxidation (creating improved crystallinity) was successful in explaining the characteristics of some films. However, an anomalous structural transition through a nearly amorphous phase occurring at a substrate bias of -40 V and film composition $ZnO_{0.78}$ remains unexplained.

Acknowledgement

The authors gratefully acknowledge financial support from the Natural Sciences and Engineering Research Council of Canada.

References

1. K. L. CHOPRA, S. MAJOR and D. K. PANDYA, *Thin Solid Films* **102** (1983) 1.
2. M. J. BRETT, R. W. McMAHON, J. AFFINITO and R. R. PARSONS, *J. Vac. Sci. Technol.* **A1** (1983) 352.
3. D. J. LEARY, J. O. BARNES and A. G. JORDAN, *J. Electrochem. Soc.* **129** (1982) 1382.
4. T. MITSUYU, O. YAMAZAKI, K. OHJI and K. WASA, *Ferroelectrics* **42** (1982) 233.
5. M. J. BRETT and R. R. PARSONS, *J. Vac. Sci. Technol.* **A4** (1986) 423.
6. *Idem, Can. J. Phys.* **63** (1985) 819.
7. S. MANIV, W. WESTWOOD and E. COLUMBINI, *J. Vac. Sci. Technol.* **20** (1982) 162.
8. C. GAWLAK and C. AITA, *ibid.* **A1** (1983) 415.
9. E. KAY, *ibid.* **A4** (1986) 462.
10. F. SARROT, Z. IQBAL and S. VEPREK, *Solid State Commun.* **42** (1982) 465.
11. J. AFFINITO, N. FORTIER and R. R. PARSONS, *J. Vac. Sci. Technol.* **A2** (1984) 316.
12. B. CULLITY, "Elements of X-ray Diffraction" Addison-Wesley, London, 1959) p. 99.
13. A. F. HEBARD and S. NAKAHARA, *Appl. Phys. Lett.* **41** (1982) 1130.
14. S. NAKAHARA and A. F. HEBARD, *Thin Solid Films* **102** (1983) 345.
15. J. A. THORNTON, *ibid.* **40** (1977) 335.

Received 3 November 1986
and accepted 28 January 1987